Annual Report of the Geological Institute of Hungary, 2003 (2004)

Tectonic analysis and structural evolution of the north-eastern Mórágy Block

GYULA MAROS[1], BALÁZS KOROKNAI[1], KLÁRA PALOTÁS[1], LÁSZLÓ FODOR[1], ANTONYINA DUDKO[1], MÁRTON FORIÁN-SZABÓ[1], LÁSZLÓ ZILAHI-SEBESS[2] and ERZSÉBET BÁN-GYŐRY[2]

[1] Geological Institute of Hungary, H–1143 Budapest, Stefánia út 14.
[2] Geo-Log Kft., H–1145 Budapest, Kolumbusz u. 17–23.

Keywords: ductile deformation, foliation, fractures, Hungary, mylonite, slickensides, South-eastern Transdanubia, structural geology, Üveghuta

Abstract

The structural evolution of the NE part of the Mórágy Granite is outlined on the basis of outcrops, about 3,500 m exploratory trenches, and nearly 60,000 measured features in about 4,200 m drilled cores. The elements measured in the cores were oriented with the help of the self-developed ImaGeo core scanner. The results are divided into magmatic, ductile, and brittle structural phases.

The primary NE–SW striking rock boundaries formed in the early evolutional stage of the Mórágy Granite Formation, during the magma-mixing processes. They preformed the "tent-like" structure of the NW- and SE-dipping features developed during the metamorphosis. In the late magmatic stage the pluton was crossed by leucocratic dykes, the orientation of which refers to NW–SE extension. After the consolidation of the magma the granitic body suffered regional metamorphosis that resulted in the formation of two NW- and SE-dipping foliation generations and narrow mylonitic zones. The mafic enclaves within the granites have rotated parallel to the foliation and been flattened. The ductile shear connected with the metamorphosis resulted in basically SSE-vergent reverse faults (and in some places their NW antithetic pairs), as well as a few strike slips. This refers to a compressional (transpressional?) tectonic regime during the ductile structural evolution.

The fractures and fracture zones were classified on the basis of their geometry, infillings, dipping, and frequency. In this paper, the structurally most significant ones will be discussed.

On the strength of the palaeostress-field analysis of the fractures bearing slickenlines, as well as the regional analogies, the following deformational events were distinguished: Cretaceous transpression, strike slip, and extension; latest Early Miocene – earliest Middle Miocene transpression (several phases); Late Miocene extension; Late Miocene – Pliocene sinistral strike slip.

The area was divided into complex regional blocks (Northern, Transitional, and Southern) on the basis of different structural features, and a tectonic map was compiled showing the major fracture zones and foliation strips. A structural evolution model was outlined concerning the present situation of the regional blocks. According to the model the neighbouring position of the regional blocks and the foliation strips can be explained by either folding, or strike slips (*i.e.* the fractured zone in the Transitional Regional Block), or the combination of these.

Introduction

The structural evaluation was outlined on the following bases: the tectonic data recorded during the drilling and ground-based exploration in 2001–2003 (MAROS et al. 2003; KOROKNAI 2003; SZONGOTH et al. 2003), the evaluation of deep boreholes drilled in the previous years (MAROS, PALOTÁS 2000a, b), and the mapping of outcrops (CHIKÁN et al. 1995; KÓKAI, SIEGL-FARKAS 2001; BALLA et al. 2003a; MAROS et al. 2003). The results achieved during the geological exploration (BALLA et al. 2003a, b; GYALOG et al. 2003) were also relied on to a great extent. The ground-based geophysical data (VÉRTESY et al. 2003a, b) were also taken into account, primarily to determine the large fracture zones.

The data system consists mainly of oriented data. In the boreholes the data were received from matching the ImaGeo core scanner images (MAROS, PALOTÁS 2000; MAROS, PÁSZTOR 2000) with the acoustic borehole televiewer images (SZONGOTH et al. 2003). This meant the orientation of about 50,000 tectonic data in respect of all boreholes. About 10,000 unoriented data derived from the non-scannable parts of the cores. About 3000 data were processed from outcrops and a further 5000 data from exploratory trenches. This meant about 70,000 data altogether.

Structural elements in connection with the magmatic evolution

In the following, the structural aspects of the monzonite–monzogranite boundaries and the orientation of the leucocratic dykes will be discussed.

Monzonite–monzogranite boundaries

During the formation of the granitic pluton, magma-mixing was going on (KIRÁLY, KOROKNAI 2004). It resulted in the formation of mafic (mainly monzonitic) enclaves within the basically monzogranitic rock body and, at the same time, monzogranite was added to the monzonites (contamination), and so hybrid rock types emerged. The boundaries of these rock types were recorded in the cores. Their distribution shows mostly NW and SE dip directions, with the NW dip direction predominating. The dip angles vary within a wide range, their maximum being about 65° (Figure 1, a).

The distribution of the contamination planes (feldspar-rich bands within the mafic rock) shows practically the same picture (Figure 1, b), with more distinct maxima. On the strength of the distributions more or less simultaneous magmatic processes can be assumed.

The orientation of the leucocratic dykes

The intrusion of leucocratic dykes (aplite, microgranite, pegmatite) probably happened at a late stage of the magmatic evolution of the pluton. On the basis of the evaluated scanned images, the presence of a few, intersecting dyke generations can be proved. The different generations, however, can be seen together only on rare occasions, so their distribution cannot be separated statistically. Their distribution (Figure 1, c) is similar to that of the monzogranite–monzonite rock boundaries, with the difference that here the SE dip direction predominates, and the dip angle is smaller — about 23°. From the distribution of the leucocratic dykes a quasi NW–SE extension can be assumed to have occured in the late stage of the magmatic evolution.

Phenomena in connection with the ductile structural evolution

This section will discuss the deformation events and the related structures that formed after the solidification of the granitic body, albeit still at a temperature that allowed the ductile deformation of the rock. This is shown in the microstructural and metamorphic mineral alterations as well (KIRÁLY, KOROKNAI 2004).

The traces of the structural changes can be studied in outcrops and boreholes, as well as in thin sections. Three planar ductile structural elements could be distinguished during the CoreDump evaluation (MAROS, PALOTÁS 2000a): steep and less steep foliations, and mylonites (see MAROS et al. 2003 for details). The effect of the ductile deformation is also reflected in the orientation and flattening of the mafic enclaves. In the following, these features are going to be discussed, and the possible structural arrangement will be touched upon on the basis of these elements.

Foliation

The most striking metamorphic phenomenon is the foliation (Figure 2) in the different rock types of the Mórágy Granite Formation, defined by the shape and oriented arrangement of the main rock-forming minerals (quartz, feldspar, biotite, and amphibole). The *mafic minerals* in the *matrix* consist of biotite and chlorite flakes or columnar amphiboles that were rotated parallel to one another by rigid-body rotation, while their inner structure changed relatively little. The *quartz* grains

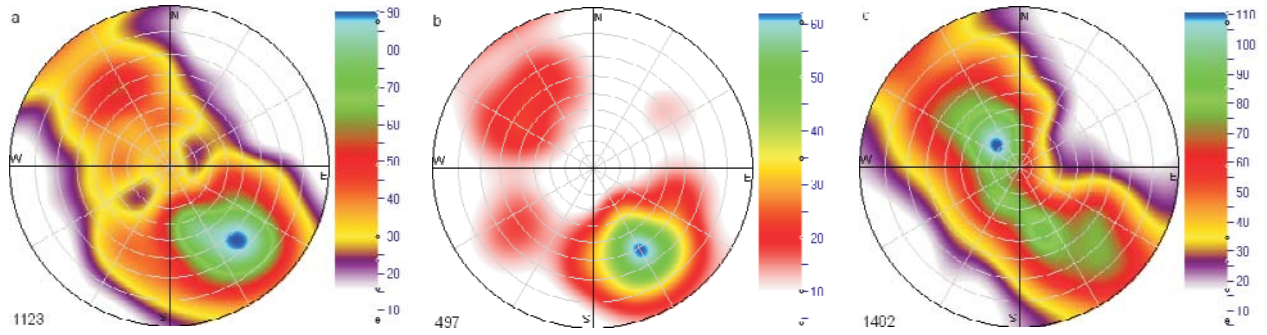

Figure 1. Pole distribution diagram of the structures related to magmatic phenomena

a – boundaries of the monzogranite and mafic enclaves, b – boundaries of contaminated monzogranite bodies in monzonite, c – leucocratic dykes. Lower hemisphere projection. The number of the evaluated planes is in the bottom left corner. The unit of the range of colours is occurence of poles

1. ábra. A magmatizmushoz kapcsolódó szerkezeti elemek pólussűrűségi diagramja

a – a granitoid és a mafikus zárványok határfelületei, b – monzonit alapkőzetben kontaminált monzogránittestek határai. c – leukokrata kőzettelérek. Alsófélgömb-vetület. A bal alsó sarokban az értékelt síkok száma. A színskála egysége darab

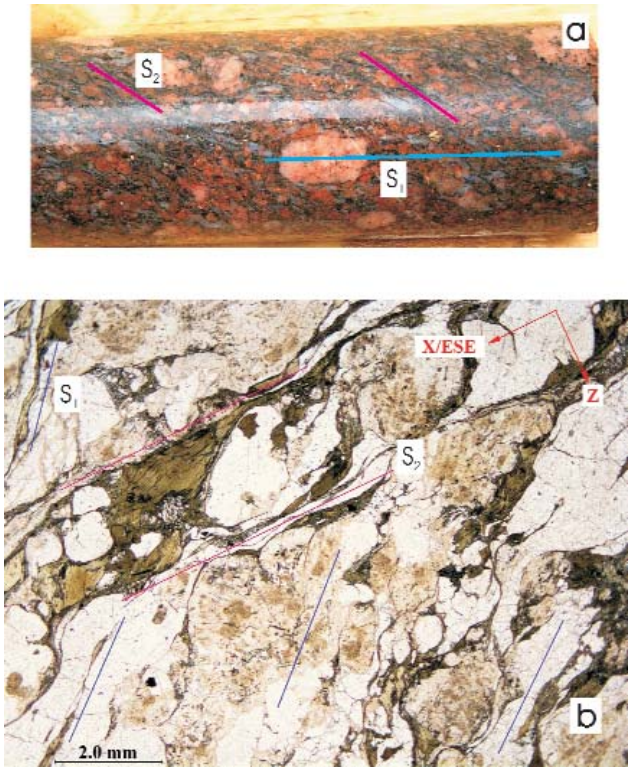

Figure 2. Core surface and microscope image of a foliated monzogranite (Üh-26, 137.7 m)

a – core surface. Two kinds of foliation can be seen on the core surface: the steep foliation (S_1) is marked by the megacrystal in the middle of the picture and the nearly horizontal, grey quartz grains on the right. The other foliation (S_2), with a dip angle of about 60° is also marked by quartz lenses as well as biotitic stripes (it is dipping to the right at the edges of the photo). b – microscope image. The steep foliation (dark blue lines) is indicated by elongated quartz lenses, feldspars, and parallel biotites organised according to the long axis. The gentle foliation (purple lines in the upper third of the photo) forms as the transposition of the steep foliation

2. ábra. Palás monzogránit magfotója és mikroszkópi képe (Üh-26, 137,7 m)

a – magfotó. A magpaláston két palásság figyelhető meg: a meredek palásságot (S_1) a kép közepén látható megakristály és a kép jobb oldalán látszó, közel vízszintes helyzetű, szürke kvarclencsék jelölik ki. A másik, kb. 60°-os dőlésű palásságot (S_2) ugyancsak kvarclencsék és biotitos sávok jelölik ki (a kép szélein közepes szöggel jobbra dől). b – mikroszkópi kép. A meredek palásságot (sötétkék vonalak) hossztengely szerint rendezett, elnyúlt kvarclencsék, földpátszemcsék és ezekkel párhuzamos biotitszemcsék jelölik ki. A laposabb palásság (lila vonalak a kép felső harmadában, S_2) a meredek palásság (S_1) transzpozíciójával jön létre

that were originally nearly isometric became flattened–elongated due to the intense intracrystalline deformation (Király, Koroknai 2004). The *feldspars* are columnar or tabular in shape, being statistically oriented in one direction according to their long axis.

The K-feldspar *mega-* and *phenocrystals* are also oriented according to their long axis, their outlines being rounded. Occasionally they are sheared or recrystallised into lenses or stripes.

Metamorphic segregation happened along the foliation planes: individual quartz, biotite, and feldspar strips formed. Definite stretching lineation along the foliation planes can be observed mainly in the mylonitic zones.

The intensity of the foliation markedly changes in space, sometimes on a cm scale. This can partly be put down to the petrological features — namely, that the larger mafic monzonitic bodies are usually not or only slightly foliated (*e.g.* Üh–27, Üh–28, Üh–37), while in other places the grain size influences the development of the foliation. On the other hand, the spatial inhomogeneity of the metamorphic effect indicates that there is a considerable difference in the strength of the foliation between boreholes drilled close to one another in mainly monzogranitic rocks (Maros et al. 2003).

Two types of foliation could be distinguished during the investigations: a steep (dip of about 80°) and a less steep (dip of about 60°, Figure 2, a, b). The latter will be called "gentle" foliation in the following, for the sake of simplicity.

Foliation generations

The average dip angle of the *steep foliation* (S_1) exceeds 75°; its dip direction is mainly to the NW or subordinately to the SE in some zones (Figure 3, a). The orientation of the foliation suggests a NW–SE compression. On the basis of the microstructural observations an intensive coaxial flattening is connected to the steep foliation. This can be best seen in the deformation of the quartz grains: the originally and approximately isometric grains change to strongly flattened, lenticular ones in the well-foliated rocks (Koroknai 2003).

In the monzogranite, *mafic enclaves* usually of oval, elongated-flattened shapes are common. Their orientation (the plane of the largest flattening, is shown in Figure 3, b) in well-foliated cores shows a strikingly good similarity to that of the steep foliation (Figure 3, a; Maros et al. 2003). The conformity of the spatial distributions of the mafic enclaves and the foliation indicates the rotation and shape change of the mafic bodies during the ductile deformation; they were "sheared" into the foliation.

In spite of the apparent effect of the ductile deformation, the deformation (elongation–flattening) of the mafic bodies is mainly of a magmatic origin — in other words, it happened when melt was still present (synmagmatic deformation). This is indicated by the presence of strongly flattened–elongated mafic enclaves in non- or weakly-deformed monzogranite. The S_1 foliation presumably superimposed on a magmatic orientation of similar position (see above), making its character even stronger.

The dip angle of the *gentle foliation* (S_2) is smaller than 75° (45–70° as a rule; Figure 3, c), and in most cases this is the foliation to be seen best in the rock. Its dip direction is usually to the NW and in some places to the SE. So, the steep and the gentle foliations generally differ from each other only in the angle of dip.

According to the thin sections and the visual observations, the gentle foliation transposes the steep foliation in various degrees, so it is younger than the steep one (Figure 2, b; Koroknai 2003). The formation of the sigmoidal quartz lenses ("worm-like quartz") can be connected to this latter deformation event, and it can be interpreted as a weak crenulation. In consequence, the two foliations represent different structural events and not the undulation of merely one foliation.

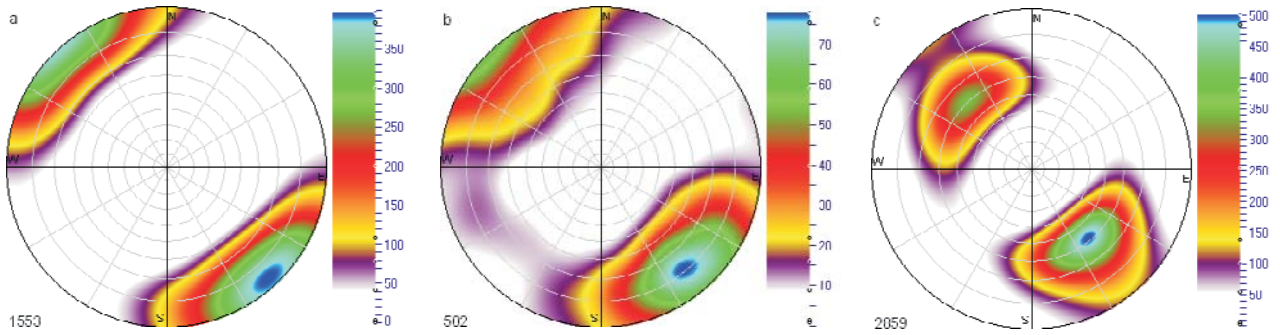

Figure 3. Pole distribution diagrams of the foliation and the monzonitic enclaves
a – steep foliation; b – flattening planes of the deformed monzonitic enclaves; c – gentle foliation. Lower hemisphere projection. The number of the evaluated planes is in the bottom left corner. The unit of the range of colours is occurerence of poles

3. ábra. A palásság és a melanokrata zárványok pólussűrűségi diagramjai
a – meredek palásság; b – a deformált melanokrata zárványok legnagyobb lapultsági síkjai; c – lapos palásság. Alsófélgömb-vetület. A bal alsó sarokban az értékelt síkok száma. A színskála egysége darab

Occasionally, asymmetric microstructures indicating to simple shear (non-coaxial deformation) can be noticed — generally showing a top-to-the SE-vergent reverse movement (GULÁCSI 2003; KOROKNAI 2003).

Foliation blocks

A few metres to a few 10s of metres long *depth blocks* can be identified along the boreholes on the basis of the variations in dip direction of the foliation (MAROS et al. 2003). Commonly, a 10–50º change in dip direction can be determined between the blocks, but on some occasions a substantial change occurs up to 180º, *e.g.* in Borehole Üh–23.

The dip direction changes within the boreholes are generally connected to fracture zones (MAROS et al. 2003). The fracture zones, however, do not automatically indicate the boundaries of "foliation" blocks. Less frequently, the change in the dip direction of the foliation can be noticed on petrographical boundaries, but this phenomenon can be noticed only within short intervals.

If one draws the dip direction distributions of the foliation on a map, *foliation strips* can be marked in the research area. The dip direction of the foliation is more or less the same within each strip (see below). Naturally, besides the characteristic dip direction other dip directions occur, too, but on the whole, these play a less important role. The determination of the strips could be reliably done in the disposal site and close to it; the continuation of the strips farther on is uncertain because of the lack of data. On the grounds of the data, three main foliation strips can be drawn in the research area (see later):

1. *Northwestern Strip*. In the northern part of the research area — north of the line of Boreholes Üh–27 – Mó–7ABCD — the dip direction of the foliation is predominantly to the NW (between WNW and N), both in the boreholes and the outcrops.

2. *Transitional Strip.* In the middle part of the research area — primarily in the zone marked by Boreholes Üh–2, Üh–22, Üh–23, Üh–25, and Üh–36 — a mixed distribution of NW and SE dip directions occur. In Boreholes Üh–3 and Üh–28 both directions occur, but here the SE dip direction dominates; this indicates a transition towards the next strip. The continuation of the transitional strip is uncertain due to the poor outcrop conditions towards ENE and WSW.

3. *Southeastern Strip.* In the southern part of the research area — marked by Boreholes Üh–4, Üh–5, and Üh–26 — foliation can be found, which dips towards the SE, and less frequently to the ESE.

South of the southern margin of the research area at Borehole Üh–26, the regional dip direction of the foliation can be determined only with great uncertainty because of the extremely low quantity of data. According to the structural data gained from outcrops, the NW dip direction seems to be more characteristic.

Mylonites

The mylonites found in the boreholes are usually between a few centimetres to a few decimetres in thickness. They show a well-developed foliation of several mm or even smaller, as well as a prominent stretching lineation on the foliation plane (Figure 4, a, b), often with a striped appearance. The direction of the stretching lineation on the foliation surface does not differ by more than 30° from the dip direction of the foliation .

Mylonites are relatively rare in the boreholes and outcrops. They occur in all main rock types as well as in the leucocratic dykes, and they usually conform to the gentle foliation. However, in some boreholes (*e.g.* Üh–22, Üh–25, Üh–27, Üh–36), they appear more frequently in the fine-grained leucocratic dykes. This suggests strong strain partitioning between the different rock types during ductile deformation.

The mylonites show significant deformation compared to their surroundings, and they appear both in rocks with none or merely weak deformation (*e.g.* Üh–27), and in rocks showing well-developed foliation (*e.g.* Üh–29).

The orientation of the mylonites is usually fairly similar to that of the gentle foliation (Figure 3, c); in most cases they are identical and this is also proved by thin section investigations.

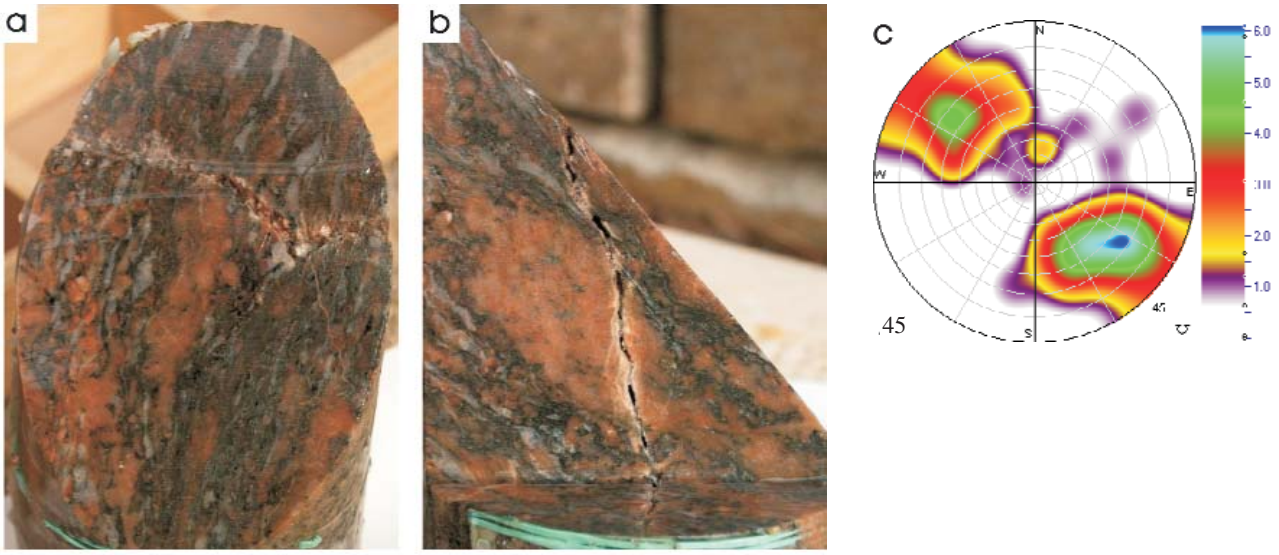

Figure 4. Hand-sized specimen of mylonitic monzogranite with polished surface (Üh-29, 140.06 m)

a – The surface is parallel to the foliation. A well-developed stretching parallel to the dip direction (roughly vertical) can be seen, marked by thin elongated quartz lenses; there are also feldspar and biotite grains (aggregates) organised according to their long axis. b – The surface is at a right-angle to the foliation and parallel with the stretching lineation. The microclin megacrystal has asymmetric tails (σ clasts) and rotated into the foliation indicates reverse shear. c – Pole distribution diagram of the mylonites. Lower hemisphere projection; the number of the evaluated planes is in the bottom left corner. The unit of the range of colours is occurrence of poles

4. ábra. Milonitos monzogránit elvágott kézipéldánya (Üh-29, 140,06 m)

a – A palássággal párhuzamosan elvágott felület. A dőlésiránnyal párhuzamos (kb. függőlegesen lefelé), kiválóan fejlett megnyúlás látható, elnyúlt vékony kvarclencsékkel, illetve hossztengely szerint rendezett földpát- és biotitszemcsék (aggregátumok). b – a minta palásságra merőlegesen és a megnyúlási vonalassággal párhuzamosan elvágott felülete. A palásságba beforgatott, aszimmetrikus uszályokkal övezett mikroklin megakristály (σ-klaszt) feltolódásos nyírást jelez. c – a milonitok pólussűrűségi diagramja alsófélgömb-vetületben. A bal alsó sarokban az értékelt síkok száma

The direction of the tectonic transport in the mylonitic zones — on the basis of the asymmetric microstructures appearing in sections perpendicular to the foliation and parallel to the stretching lineation — seems to be mostly a SE. Rarely SSE-vergent reverse movement, associated with a slight to moderate strike-slip component in some places (Koroknai 2003; Gulácsi 2003). The NW-vergent reverse movements detected in the SE dipping mylonitic foliation can be interpreted as antithetic pairs. Structures referring to such displacements can sometimes be observed on the planes of the gentle foliation, too.

In some instances, sinistral and dextral strike-slip shear is also evident. This could be of the same age as the reverse movements, but there are no direct observations to prove this. In rare cases, traces of ductile shear can also be observed on the planes of the steep foliation (S_1): these are normal faults and most probably precede the shear events discussed above, but more data are needed to prove this.

Phenomena connected with the brittle structural evolution

It was clear when the investigations started that a large number of brittle deformational events have to be considered, and that the overlying sediments cannot be counted on to help with the timing of the deformational phases. Because of this, in the first stage of the evaluation the fractures were classified only on a phenomenological basis (Maros et al. 2003). First the large fracture zones, then the fractures bearing slickenlines, and finally the lithoclases were separated. The latter two were classified according to their geometry, their relationship to one another, infillings, openness, and the alteration they caused in the neighbouring rock. The depth and areal distributions of the fracture groups were analysed. This classification, however, does not make it possible to determine the deformational events that have resulted in numerous fracture generations and the succession of these events. At the same time, the reconstruction of the brittle structural evolution of the granitic body cannot be done without clearing up the succession of the structural events; in fact this may be its most important element. In the following, a short summary will be given about the main characteristics of the fracture pattern. Then the following will be presented: stress fields determined by slickenlines and some distinguishable fracture sets, and the results gained by the analysis of the regional distribution of the most important structural features.

Fractures

In the following, the description and the spatial distribution of all the fractures, the open fractures, the cataclasites, the trachyte dykes, the fractures with accompanying reddening, and the slickenlines will be dealt with.

All fractures

During the evaluation of all fractures (Figure 5) about 46,800 data coming from the tectonic evaluation (Maros et

al. 2003), and about 30,100 data deriving from the acoustic borehole televiewer evaluation (SZONGOTH et al. 2003) were taken into account.

The distribution of the *tectonic data* (Figure 5, a) — although it shows the characteristic strike directions of the area — gives a NE main dip direction. The huge amount of data is divided evenly between the maxima: there is only a 1.5 times difference between the dark blue and yellow maxima, so the number of both the ENE–WSW striking and the steep S dipping fractures (about 4,000) is significant. The most frequent dip angles in the pole distribution diagram corrected by the Terzaghi-correction are between 70–80°.

The distribution of the *borehole televiewer data* (Figure 5, b) shows two maxima with NE–SW strike. Besides these, a less significant E–W maximum-pair also appears. The fractures with less than 40° dip angles fall into the SE quarter of the diagram.

The two distributions are fairly similar, but the NE dipping maximum is dominant only in the tectonic data. The causes of the difference will have to be revealed by further investigations. Among the possible explanations are the following:

In the tectonic database the major amount of data comes from the evolution of the scanned images. The resolution of the core scanner is more than 50 times the resolution of the acoustic borehole televiewer. It is possible that most of the fractures dipping NE are hair-cracks that are invisible for the acoustic borehole televiewer. On the other hand, the tectonic database contains a great many data from outcrops and exploratory trenches. Thus the difference between the number of data also means a difference in the origin of data. The third factor to be taken into consideration is the slight difference between the methods used to visualise the distribution of data; this causes the more blurred borehole televiewer distribution picture and the more distinct tectonic distribution picture. The Terzaghi correction can also have a different effect on the blurred and distinct maxima.

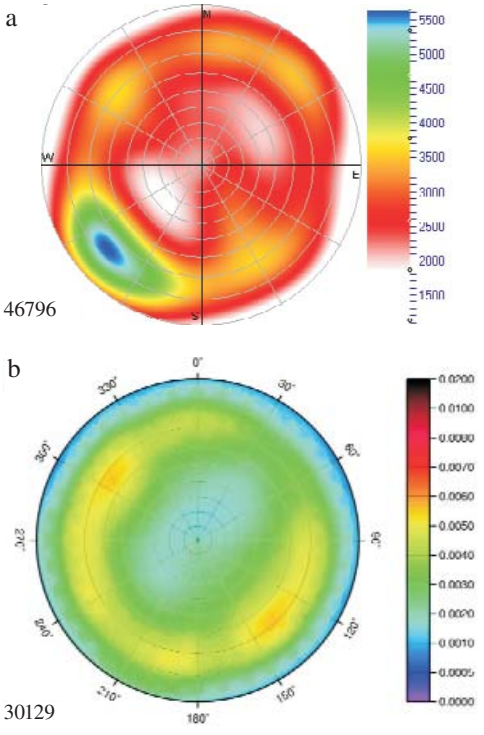

Figure 5. Pole distribution diagram of the fractures
a – tectonic evaluation; b – borehole televiewer evaluation. Lower hemisphere projection. The number of the evaluated planes is in the bottom left corner. The unit of the range of colours is occurrence of poles in Figure a and their proportion in Figure b

5. ábra. Az összes törés pólussűrűségi diagramja
a – a tektonikai, b – a lyuktelevíziós értékelés alapján. Alsófélgömb-vetület. A bal alsó sarokban az értékelt síkok száma. A színskála egysége az a ábrán darab, a b ábrán hányad

Open fractures

Open fractures are the ones that were open in their original place (Figure 6). Due to the lack of possibility of direct observation, the recognition of this feature implies subjectivity. During the tectonic evaluation this subjectivity derived from the fact that the evaluating geologist could see the cores only in the core boxes, after the drilling process. Due to the strain, the originally closed fractures might have become open during the drilling. The distinction between closed and open fractures was based on some characteristic features of the fractures. The fractures with a seemingly fresh fracture surface or with fitting infillings were considered to have been closedoriginally. The group of open fractures comprises the remaining lot. Two main fracture groups, NE and NW dipping ones respectively, proved to be open (Figure 6, a), the latter group having a dip angle between 20–25°.

During the *borehole televiewer* evaluation, the criterion for a fracture being open was that the fracture be present both on the traveltime and the amplitude images. This is because on the traveltime image only those fractures appear that are microcavernous and the traveltime of the acoustic waves increases. In the amplitude image, fractures that are mechanically different from the neighbouring rocks also appear. The result of this evaluation can be seen in Figure 6, b.

The two distributions are fairly similar in respect of azimuth. Most maxima appear in both diagrams, although this time the tectonic distribution shows a more blurred image. The main difference is at the low-angled fractures, and particularly at the fractures dipping NW. The latter are not open according to the borehole televiewer image. These are either closed in the borehole or their openness is below the resolution of the traveltime image.

Some of the open fractures appear as a whole sine (Figure 6, c). They represent about 25% of all fractures (2441 occurrences) according to the borehole televiewer evaluation, and the fractures dipping SE predominate. The ratio of the fractures dipping NW is about the same as with all the open fractures (on the basis of the borehole televiewer image). The distribution exhibits a striking similarity to the gentle foliation.

Cataclasites

This deformation phenomena forms a transition between the ductile and the brittle deformation regimes. This — probably very complex — group contains the cataclasite

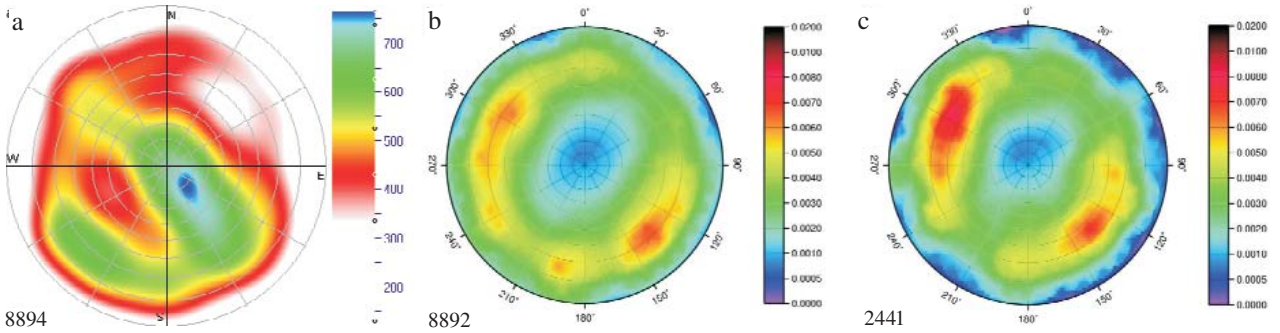

Figure 6. Pole distribution diagram of the open fractures

a – tectonic evaluation; b, c – borehole televiewer evaluation: b – all open fractures; c – whole sines. Lower hemisphere projection. The number of the evaluated planes is in the bottom left corner. The unit of the range of colours is occurrence of poles in Figure a and their proportion in Figure b and c

6. ábra. A nyílt törések pólussűrűségi diagramja

a – tektonikai, b, c – lyuktelevíziós értékelés alapján: b – összes nyílt törés, c – teljes szinuszt adó nyílt törések. Alsófélgömb-vetület. A bal alsó sarokban az értékelt síkok száma. A színskála egysége az aábrán darab, a b és c ábrán hányad

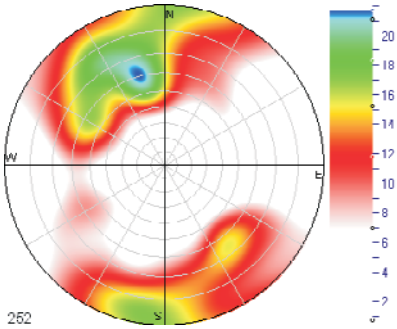

Figure. 7. Pole distribution diagram of the planar boundaries of the cataclasites and the "quasi ductile" planes

Lower hemisphere projection. The number of the evaluated planes is in the bottom left corner. The unit of the range of colours is occurrence of poles

7. ábra. A kataklázitos kőzetszakaszok síkszerű határainak és a „kvázi-képlékeny" síkok pólussűrűségi diagramja

Alsófélgömb-vetület. A bal alsó sarokban az értékelt síkok száma. A színskála egysége darab

zones and what are called quasi-ductile zones with planar boundaries. The latter phenomenon is a shear zone or joined shear zones that are a few centimetres thick in the cores and often a few decimetres in the outcrops. Within the shear zones the rock and the infillings often show a "mylonite-like" striped, sometimes sigmoidal appearance. In thin sections, the dynamic recrystallisation of the calcite infillings can sometimes be noticed. The pole distribution diagram of these planes shows that this feature can be associated with steep planes (Figure 7). The distribution picture is quite complex: it shows E–W and NE–SW striking and rather steep planes, probably conjugate pairs. The S and SE dipping planes predominate in both groups. The former conjugate pair is presumably associated with palaeostress field F_1 (see below); the origin of the latter pair needs further investigations.

Trachyte dykes

The strike of the trachyte dykes is very similar to the strike of the Mecsekalja Zone but crosses it at a low angle (Balla et al. 2003b). Such dykes were crossed in Boreholes Üh–27 and Üh–29 besides some outcrops. The distribution of the boundaries of such dykes from Borehole Üh–29 is shown in Figure 8, a. By means of the fractures bearing slickenlines, the intrusion of the dykes can probably be associated with the extensional stress field F_5 (see below). The latter probably initiated the intrusion of the dykes. The distribution of the fractures that cross the dykes (Figure 8, b) shows parallel strike with that of the dykes.

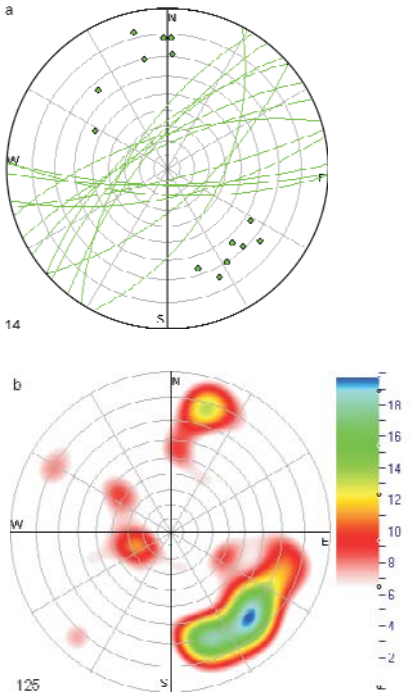

Figure 8. Distribution of the trachyte dykes crossed in the boreholes and the fractures cutting the dykes

a – stereogram of the trachyite dykes; b – pole distribution diagram of the fractures cutting the dykes; the unit of the range of colours is occurrence of poles. Lower hemisphere projection. The number of the evaluated planes is in the bottom left corner

8. ábra. A mélyfúrásokban harántolt trachit-telérek és a bennük észlelt törések eloszlása

a – trachit-telérek sztereogramja; b – a bennük észlelt törések pólussűrűségi diagramja. Alsófélgömb-vetület. A bal alsó sarokban az értékelt síkok száma. A színskála egysége darab

Fractures with accompanying reddening

According to the analysis of the succession of the fractures and infillings (MAROS et al. 2003), the fractures accompanied by secondary reddish colouring (Figure 9) can be associated with one of the earliest brittle deformations. The distribution of these fractures is fairly homogeneous, with a dip direction to the NE and a dip angle of about 65°. These fractures probably formed in stress field F_3 (see below).

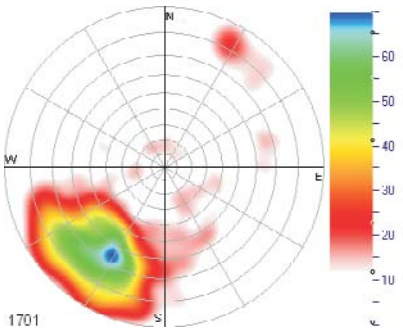

Figure 9. Pole distribution diagram of the fractures with accompanying reddening

Lower hemisphere projection. The number of the evaluated planes is in the bottom left corner. The unit of the range of colours is occurrence of poles

9. ábra. A kivörösödött szegéllyel rendelkező törések pólussűrűségi diagramja

Alsó-félgömb-vetület. A bal alsó sarkokban az értékelt síkok száma. A színskála egysége darab

Fractures with slickenlines

From the spatial analysis or the comparison, to theoretical brittle deformation models of these slickenlines as displacement vectors, one can deduce the orientation and nature of former stress fields, as well as the pattern of the resulting brittle deformation (ANDERSON 1951; ANGELIER 1984).

Altogether 885 fault planes bearing slickenlines were observed, of which 152 (17%) could not be determined. These could not be involved in the palaeostress-field calculations.

Six stress fields could be traced in the Site area and its surroundings. The individual stress fields are characterised by the orientation of the two horizontal stress axes. The orientations and characters that are typical of the stress fields are summarised in Table 1.

An examination carried out to determine whether the infilling types in the fractures can be associated with the fracture system of a characteristic stress field. It turned out that the hydrothermal infillings occur in about the same ratio in the main palaeostress-field directions; thus the fractures associated with a certain structural phase do not have characteristic hydrothermal infilling. The trachyte dykes have been shown to be the only exception to this; they entered such tensional or tensional–shear fractures that could have formed in stress field F_5.

Division of the research area

In the following section the results coming from the distribution of the different structural phenomena will be introduced.

Complex blocks

The research area was divided according to of the fracture distributions. After correlation with the magmatic and ductile deformation phenomena, this resulted in structurally well-

Table 1. Characteristics of the palaeostress fields

Stress field	Character of stress field	Main stress direction	Characteristic strikes and dip angles of fractures	Nature of displacement
F_1	strike-slip	σ_1 = WNW ESE	N060-085E/75-90°	dextral strike slips
			N130 160E/80 90°	sinistral strike slips
F_2	strike-slip	σ_1 = NNW SSE	N095 130E/60 90°	dextral strike slips
			N010-045E/45-90°	sinistral strike slips
			N050-080E/25-55°	reverse faults
F_3	strike-slip and extensional	σ_1 = NW SE σ_3 – NNE-SSW	N130-150E/50-75°	normal faults
			N340-020E/75-90°	sinistral strike slips
			N070 090E/75-90°	dextral strike slips
F_4	strike-slip and compressional	σ_1 – NNE-SSW σ_3 = ESE WSW	N025 055E/25 80°	sinistral strike slips
			N130-175E/65-90°	dextral strike slips
			N100-125E/20-50°	reverse faults
			N020 040E/55 75°	normal faults
F_5	extensional	σ_3 SE-NW	N010 055E/45 80°	normal faults
F_6	compressional and strike-slip	σ_1 = ENE WSW	N085 120E/60 90°	sinistral strike slips
			N015 045E/80 90°	dextral strike slips
			N015-045E/55-75°	dextral strike slips
			N000-030E/15-45°	reverse faults

separated complex regional blocks (Figure 10). The regional blocks were divided in the research area into smaller blocks and these were then separated by fracture zones. Because of this, different sections of a borehole may fall into different blocks. The boundaries of the regional blocks were defined according to the most significant changes — namely, by the determined or assumed fracture zones running along the boundaries of the foliation strips. This is because it was found that the foliation strip boundaries are indicated by fracture zones in the boreholes. The strip boundaries in many cases can be well correlated with certain fracture zones.

The *Southern Regional Block* in the SE part of the research area is characterised predominantly by a SE dip direction that is typical of Boreholes Üh–4, Üh–5, and Üh–26. All the respective distributions of the rock boundaries, leucocratic dykes, foliations, and fractures show a SE maximum.

The *Transitional Regional Block* is represented by Boreholes Üh–2, Üh–3, Üh–22, Üh–23 below 105 m, Üh–25, Üh–28, Üh–30, and Üh–36, as well as the whole Trench A1 and partly Trench A2. This is the regional block that contains the bundle of fracture zones that divide the Northern and the Southern Regional Blocks. Within this region the rock bodies within fracture zones are referred to as "blocks" and they can be characterised by diverse fracture distributions. Within the Transitional Regional Block, with regard to the fracture distributions, two parallel striking belts can be distinguished. The first one, in the south, includes Boreholes Üh–2, Üh–3, Üh–22, Üh–28, and Üh–30, and the fracture distribution shows a strong similarity to that of the Southern Regional Block; however, besides the SE dip direction, NNW and NE directions also occur. The other belt contains Boreholes Üh–23 below 105 m, Üh–25, and Üh–36. Here the fracture distribution is similar to that of the Northern Regional Block with the predominance of NE and NW dip directions. The distribution of the rock boundaries, the leucocratic dykes, and the foliation also correlates with

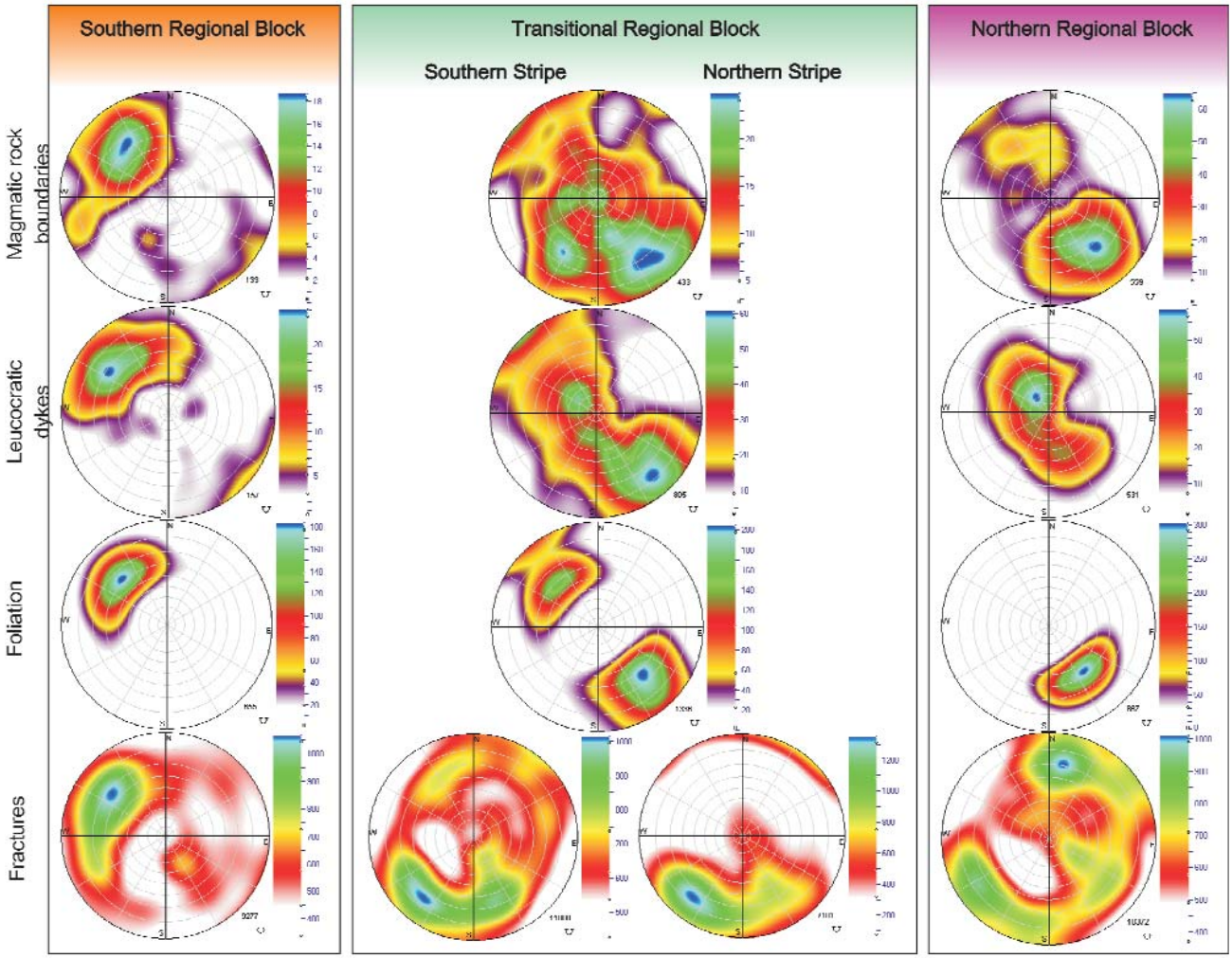

Figure 10. The regional blocks and the pole distribution diagrams of the features showing characteristically different distributions
Lower hemisphere projection. The number of the evaluated planes is in the bottom right corner. The unit of the range of colours is occurrence of poles

10. ábra. A tektonikai tömbök és a különböző eloszlású jelenségek pólussűrűségi diagramjai
Southern Regional Block = Déli Regionális Tömb, Transitional Regional Block = Köztes Regionális Tömb, Northern Regional Block = Északi Regionális Tömb, Southern Stripe = Déli pászta, Northern Stripe = Északi pászta, magmatic rock boundaries = magmás kőzethatárok, leucocratic dykes = leukokrata telérek, foliation = palásság, fractures = törések. Alsófélgömb-vetület. A jobb alsó sarkokban az értékelt síkok száma. A színskálák egysége darab

the mixed distribution of the fractures: the characteristic directions of both the Southern and the Northern Regional Blocks are present (Figure 10).

The *Northern Regional Block* is represented by basically NE dipping fracture sets in Boreholes Üh–23 above 105 m, Üh–27, Üh–29, Üh–31, Üh–32, Üh–33, Üh–34, Üh–35, and Üh–37, as well as the NW section of Trench A2. Besides the main fracture direction, NE–SW striking, about 45° NW dipping fractures occur, too. Another important fracture group is dipping to the S–SSW at an angle of about 80°.

The dip directions of both the foliation and the rock boundaries are to the NW. The distribution of the leucocratic dykes show both NW and SE dip directions.

Tectonic map

The tectonic map (MAROS et al 2003) of the region was compiled on the basis of the larger fracture zones and the regional blocks (Figure 11, a). The dip of the larger fracture zones was recognized in exploratory trenches and deep boreholes. Their position was specified by ground-based

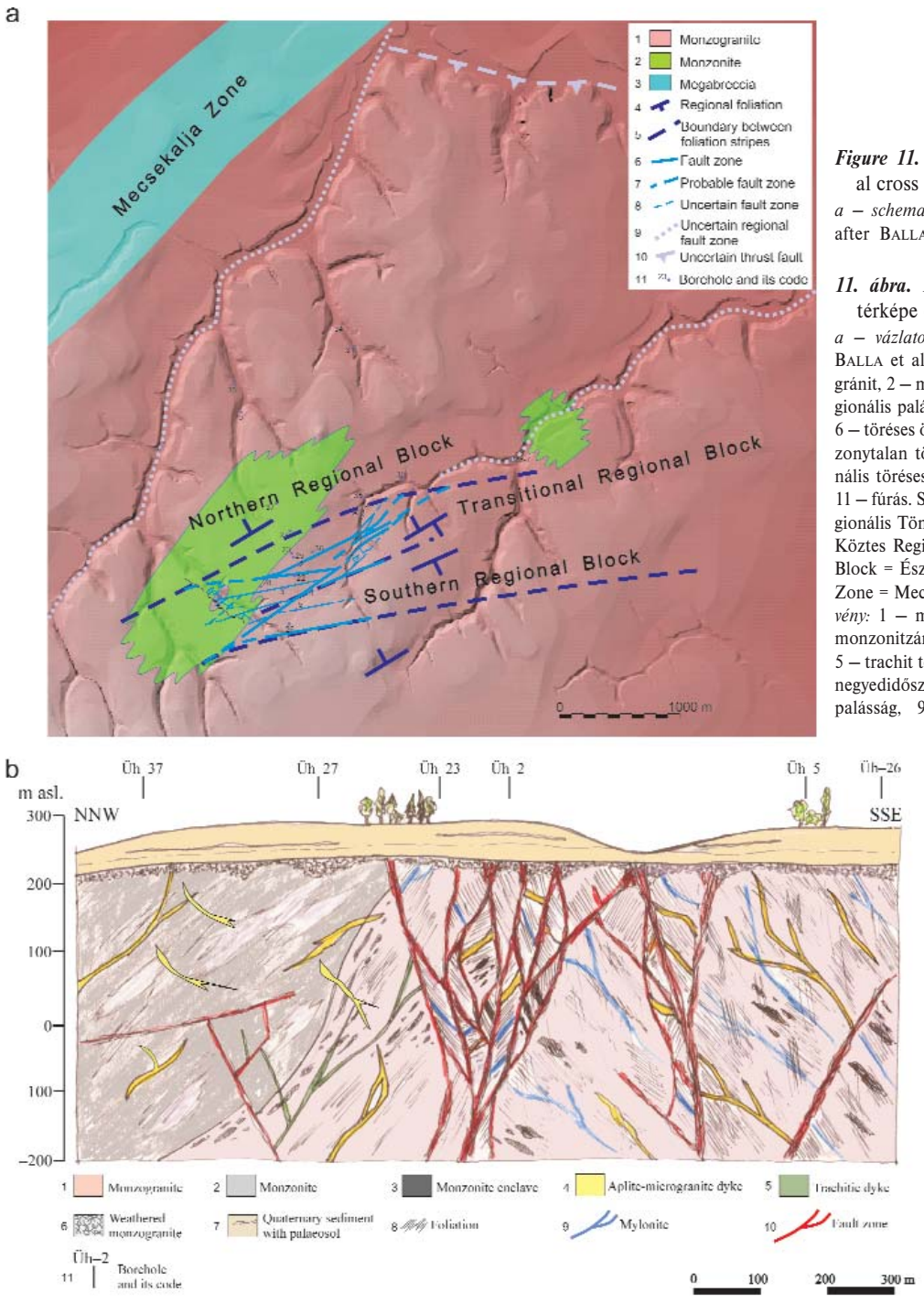

Figure 11. Tectonic map and conceptual cross section of the research area
a – schematic tectonic map (basement map after BALLA et al. 2003b); *b – conceptual cross section*

11. ábra. A kutatási terület tektonikai térképe és koncepcionális szelvénye
a – vázlatos tektonikai térkép [aljzattérkép BALLA et al. (2003b) nyomán]: 1 – monzogránit, 2 – monzonit, 3 – megabreccsa, 4 – regionális palásság, 5 – palássági pászta határa, 6 – töréses öv, 7 – valószínű töréses öv, 8 – bizonytalan töréses öv, 9 – bizonytalan regionális töréses öv, 10 – bizonytalan feltolódás, 11 – fúrás. Southern Regional Block = Déli Regionális Tömb, Transitional Regional Block = Köztes Regionális Tömb, Northern Regional Block = Északi Regionális Tömb, Mecsekalja Zone = Mecsekalja-öv. *b – koncepcionális szelvény:* 1 – monzogránit, 2 – monzonit, 3 – monzonitzárvány, 4 – aplit-mikrogránit telér, 5 – trachit telér, 6 – mállott monzogránit, 7 – negyedidőszaki üledék paleotalajszinttel, 8 – palásság, 9 – milonit, 10 – törésesöv, 11 – fúrás és jele

and well-logging methods, and their dip directions were determined with the help of acoustic borehole televiewer data. Their length, connectivity, and geometry were determined by means of hydrodynamic single-hole and interference tests (BALLA 2003; BALLA et al. 2003b, 2004).

Some problems arose with respect to: the possible continuation of the fracture zones, their termination at another zone, or the intersection of different zones. To solve these problems a simplified fault pattern was used as a possible structural model. It is important to stress that although this model is in agreement with the data derived from the boreholes and exploratory trenches, as well as the palaeostress-field analysis, it is still only a model. Consequently, besides the uncertainty about the exact geometry of the fracture zones, their linking to one another and the places of their intersections are hypothetical and may change after further refinement. In Figure 11, b, a NW–SE striking conceptual cross section is presented, and this introduces the main characteristics of the regional blocks.

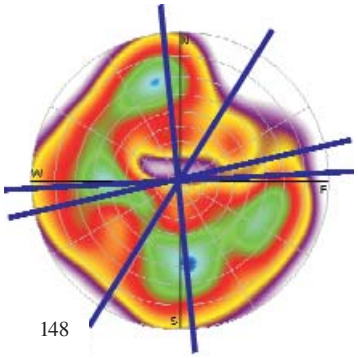

Figure 12. Distribution of the main fracture zones

Blue lines = strikes of main fracture zones; dark blue colour on the diagram = largest pole density; purple = smallest pole density. Lower hemisphere projection. The number of the evaluated planes is in the bottom left corner. The unit of the range of colours is occurrence of poles

12. ábra. A nagyobb töréses övek irányeloszlása

Kék vonalak = fő törésesöv-irányok; a diagramon sötétkék szín = legnagyobb pólussűrűség, lila = legkisebb pólussűrűség. Alsófélgömb-vetület. A bal alsó sarokban az értékelt síkok száma. A színskála egysége darab

Structural evolution

In the following, the structural evolution of the Mórágy Granite will be sketched out.

Deformation events

Phase D_0 (Palaeozoic). The development of the orientation that is characteristic of practically all geological-structural phenomena in the research area started as early as the magmatic evolution. The basically NE–SW strike of the boundaries between the granite and the mafic enclaves could have developed then. This magmatic orientation and the flattening–elongation of the mafic enclaves during the magmatic evolution suggest that the formation of the pluton happened under stress (synmagmatic deformation). The leucocratic dykes intruded the already consolidated pluton (KIRÁLY, KOROKNAI 2004) as a result of a NW–SE extension.

Phase D_1 (Carboniferous?). During the ductile deformation that superimposed on the primary magmatic orientation, the developing steep foliation (basically coaxial flattening) made the original orientation even more significant.

Phase D_2 (Carboniferous?). The steep foliation was overwritten by a less steep (gentle) foliation, and mylonitisation took place in narrow shear zones.

The exact timing of the metamorphosis and the attendant ductile deformation events have not yet been solved. According to the radiometric data, the age of these events is about 320(–300?) Ma (BALOGH et al. 1983; LELKES-FELVÁRI et al. 2000; TÜSKE 2001; CSERNÜSOV et al. 2003).

On the basis of the relative succession of the brittle elements and literature analogies, the brittle deformation history was reconstructed and deformation phases were set up. To do this, the evaluation of the palaeostress fields and the distribution of the major fracture zones were used (Figure 12). By means of the distribution of the fracture zones, the possible kinematics of the simplified fault pattern of the research area was given. On the basis of new observations and the published structural results concerning the Mecsek and Villány Mts. (see below in detail), it is clear that more than one phase can be characterised by fairly similar or identical stress fields — that is, certain stress fields recur during the structural evolution. So some fractures must have been reactivated with identical kinematics several times.

Phase D_3 (Middle Cretaceous). The brittle deformation history can be traced from the Middle Cretaceous (Figure 13), but the existence of earlier fractures cannot be excluded. The oldest fractures can be connected to folding or thrusting and this can also be seen both in the Mecsek and the Villány Mts. These fractures formed as a result of a NW–SE compression (WÉBER 1977; BENKOVICS et al. 1997). Any of the determined stress fields F_1, F_2 and/or F_3 could have characterised this phase, changing over time or space. It is possible to calculate such changes mainly with reverse movements parallel to the foliation and joint strike slips that occured during this phase (kinematics "α"). The area was then affected by transpressional deformation. Presumably, the first, gently dipping, carbonate–haematite infillings as well as the thick, calcite, dolomite, ankerite infillings, and the reddenings determined by CoreTime evaluation can be ranked in this phase. The analogous stress field, which appears in Erdősmecske, was not detected by BERGERAT and CSONTOS (1988) in Miocene rocks and this supports the idea that it is of pre-Miocene age.

Phases D_4 and *D_5 (Late Cretaceous).* The next phase D_4 of the deformation history could be the reactivation of stress field F_4, which moved NE–SW striking sinistral strike slips (kinematics "β"). The fractures that can be well identified in the Bátaapáti (Üveghuta) region are similar to other important strike slips in the Mecsek–Villány region. One example is the Büdöskút Zone in the western part of the Mecsek Mts, where a similar stress field was identified

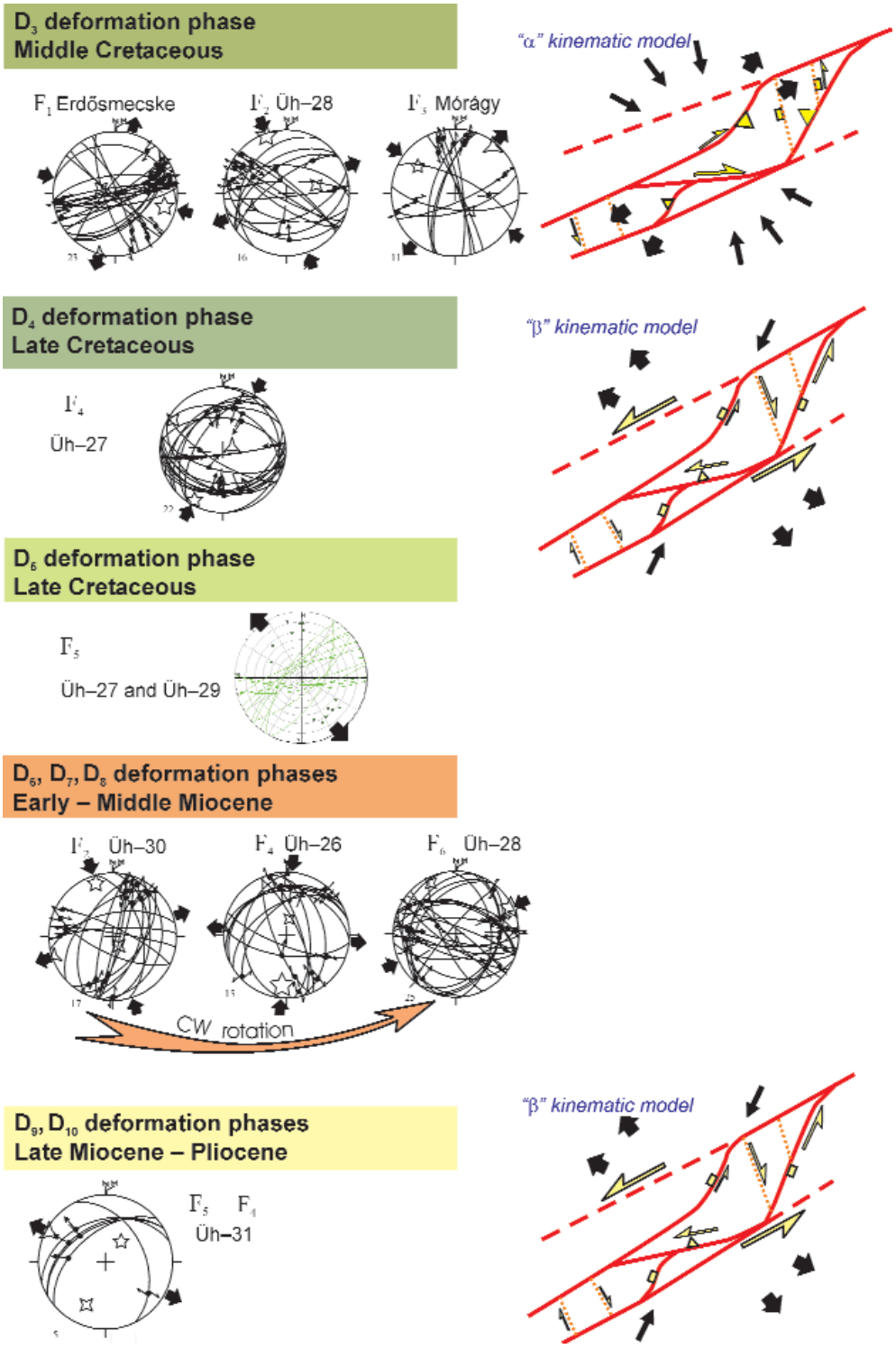

Figure 13. Brittle deformation phases reconstructed by means of the palaeostress-fields

In the *diagrams* Fx = number of palaeostress fields (see in Table 1); CW = clockwise; five-pointed star = σ_1; four-pointed star = σ_2; three-pointed star = σ_3; black arrow = stress direction. In the *kinematic models* red line = fracture zone; dashed red line = strike of displacement zone; dotted orange line = secondary fracture zone; yellow rectangle = normal fault; yellow triangle = reverse fault; one-sided yellow arrow = strike slip. The nature of displacement along the fractures in the kinematic models ("α" and "β") was determined by the given stress field. The stereograms are in a lower hemisphere projection.

13. ábra. A paleo-feszültségterek alapján rekonstruált töréses deformációs fázisok

A *feliratokban* deformation phase = deformációs fázis, kinematic model = kinematikai modell, Middle Cretaceous = középső kréta, Late Cretaceous = késő-kréta, Early-Middle Miocene = kora-középső-miocén, Late Miocene - Pliocene = késő-miocén-pliocén. A *diagramokon* F_x = paleo-feszültségtér sorszáma (l. az 1. táblázatban), CW = óramutató járásával azonos irányú, ötágú csillag = σ_1, négyágú csillag = σ_2, háromágú csillag = σ_3, fekete nyíl = feszültségirány. A *kinematikai modelleken* piros vonal = töréses öv, szaggatott piros vonal = elmozdulási zóna fő csapása, pöttyözött narancssárga vonal = másodrendű töréses öv, sárga téglalap = normál vető, sárga háromszög = feltolódás, féloldalas sárga nyíl = eltolódás. A deformációs fázisokhoz tartozó kinematikai modellekben („α" és „β") a törésmintázat töréseinek elmozdulás típusait az adott feszültségtér határozza meg. A sztereogramok alsófélgömb-vetületben készültek

(MAROS et al. 2000). The sinistral nature of the Zone is supported by previous research (KONRÁD 1998; HÁMOS 1990) and new measurements, too. This could have closed down at the end of the Cretaceous by the extensional deformation D_5. The latter was caused by stress field F_5 and is best marked by the intrusion of magmatic dykes in the Bátaapáti (Üveghuta) region.

Phases D_6, D_7, and *D_8 (Early–Middle Miocene).* The brittle deformation at the end of the Early Miocene and the beginning of the Middle Miocene was linked with the clockwise rotation of the rocks (MÁRTON, MÁRTON 1999). As a consequence of the rotation stress fields F_6, F_4, and later F_2 affected the rocks. The rapid kinematic–dynamic change, however, is apparent in the sense that it could be the result of the rotation of the blocks in a stable stress field (CSONTOS, BERGERAT 1993; FODOR et al. 1999). The changing stress field could have induced displacements of different kinematics during phases D_6, D_7, and D_8. The sinistral transpressional displacements shown in the Mecsek Northern Thrust Zone belong to here (TARI 1993).

Phases D_9 and *D_{10} (Late Miocene – Pliocene).* CSONTOS et al. (2002) suggest an extensional stress field with a NW–SE axis at the beginning of the Late Miocene. With such features deformation phase D_9 corresponds to stress field F_5 in the area. The transpressional emergence of the Mecsek and the Villány Mts. started at the end of the Miocene, and this initiated reverse strike slips (WEIN 1965; CSONTOS et al. 2002). This sort of deformation (D_{10}) can be found in the larger environment of the Site, in certain parts of the Mecsekalja Zone (KLEB 1973; NÉMEDI VARGA 1983). Within the investigated Üveghuta area the previously-formed brittle elements and foliation planes were reactivated in the main NE–SW striking sinistral strike-slip zone (kinematics "β"), and a large number of often open fractures were formed. The branching–interwining fracture system was most probably transtensional and moved under the influence of stress field F_5 and to a lesser extent F_4.

Development of the present structural pattern

The adjoining situation of the regional blocks and blocks showing different structural features are discussed here. The Northern and Southern Regional Blocks are considered more or less undisturbed, uniform units, while the Transitional Regional Block is considered as a mass of blocks of different spatial origin. To explain this, two structural solutions and their combination can be considered.

In the *first possible solution,* folding formed the tent-like structure of the dip directions in the Northern and Southern Regional Blocks. This also explains the position of the metamorphic sandstone–siltstone flakes in the granite. The different foliation strips stand for the wings of the folds. In this case, relatively tight folds have to be taken into account to explain why transitional (fairly flat) foliation cannot be observed anywhere. The upper part of the hinge zones with transitional dips could have been ruined by later erosion. However, this model does not give a good explanation about the irregular (foliation, *etc.*) which characterises of the blocks in the Transitional Regional Block.

As a *second possible solution*, the Transitional Regional Block is considered to be a strike-slip zone, where differently orientated parts of the original pluton are placed next to one another. In this case distant blocks of the original pluton were brought together by the strike slips (Figure 14, d).

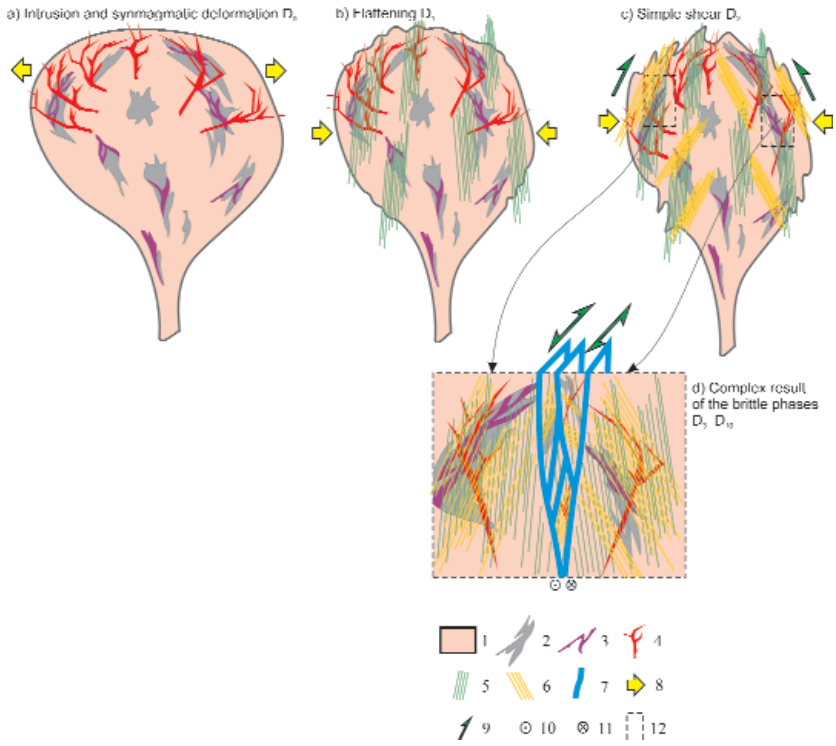

Figure 14. Schematic model of the structural evolution of the Mórágy Formation

1 – monzogranite, 2 – monzonite, 3 – monzogranite infiltration within monzonite, 4 – aplite-microgranite dyke, 5 – steep foliation, 6 – gentle foliation, 7 – fracture zone, 8 – direction of tension or extension, 9 – shear, 10 – approaching block, 11 – receding block, 12 – supposed original position of the regional blocks in the pluton; the dashed line indicates that this can be in front of or behind the plane of the figure. During D_3-D_{10} the different parts of the pluton were placed next to one another by sinistral strike slips

14. ábra. A Mórágyi Formáció szerkezeti fejlődésének sematikus modellje

A D_3-D_{10} során a pluton különböző részei balos eltolódásokkal kerültek egymás mellé. 1 – monzogránit, 2 – monzonit, 3 – monzonitos környezetben monzogránit-beszűrődések, 4 – aplit-mikrogránit telér, 5 – meredek palásság, 6 – lapos palásság, 7 – töréses öv, 8 – nyomás- vagy húzásirány, 9 – nyírásirány, 10 – közeledő blokk, 11 – távolodó blokk, 12 – a tömbök feltételezett eredeti helyzete a plutonban (a szaggatott körvonal jelzi, hogy ez a hely a részábra síkja előtt, illetve mögött is lehet). A *feliratokban*: intrusion = benyomulás, flattening = lapulás, simple shear = egyszerű nyírás, complex result of the brittle phases = a töréses események együttes eredménye

The combination of the two models was also taken into consideration and this explains the different characteristics (besides the magmatic preformation and the coaxial flattening) of the blocks with folding; it also presumes strike slips in the Transitional Regional Block.

It is important to note for all hypotheses that the area covered by the regional blocks is too small to enable conclusion to be made about the exact genetics of the blocks.

Conclusions

The primary, NE–SW striking boundaries of the different rock types were formed in the early magmatic evolution phase of the Mórágy Granite Formation, during magma mixing (PITCHER 1997). This latter it preformed the NW and SE dipping tent-like structure that developed during the metamorphosis. This process probably took place under the effect of a stress field (synmagmatic deformation). Even then, a NE–SW elongated pluton can be reckoned with to have existed since no perpendicular monzonite–monzogranite boundaries or dykes can be detected in large number. Figure 14 illustrates the cross section of the pluton. Later, in the late phase of the magmatic evolution, acidic dykes intruded the granitic body, probably in a NW–SE extensional stress field. At least one part of the dykes is supposedly concentric and followed the shape of the pluton and the synmagmatic preformation besides the stress field (CASTRO, FERNANDEZ 1998). Of course, additional radial dykes crossing the boundary of the pluton could also be present.

The Mórágy Granite Formation suffered regional metamorphism during the *Variscan orogeny*. This is reflected in the following ductile deformation events:

D_1: Formation of a usually NW dipping steep (>75°) foliation (S_1) associated with intensive coaxial flattening (Figure 14, b). The setting of the foliation indicates roughly NW–SE compression.

D_{2a}: Formation of a "gentle" (~65°) foliation (S_2) which crenulates–transposes the steep foliation to various degrees, but their dip directions are in agreement (Figure 14, c).

D_{2b}: Formation of narrow mylonitic zones characterised by top-to-the-SSE (rarely N)-vergent reverse movements. The orientation of the mylonites generally corresponds to that of the gentle foliation (S_2).

During the ductile deformation, the monzonite enclaves rotated parallel to the foliation and suffered flattening. The ductile shear events are predominantly top-to-the-SSE-vergent reverse movements (or in some places their antithetic equivalents to the NW), but strike slips also occur, albeit rarely. As a whole, these phenomena indicate a compressional (transpressional?) tectonic regime.

The deformation history of the *Alpine orogeny* was reconstructed on the basis of palaeostress fields calculated from slickenlines and their regional analogies.

D_3: Cretaceous transpression with reverse faults parallel to the foliation and joint strike slips.

D_4: Cretaceous strike-slip stress field with NE–SW striking sinistral strike slips.

D_5: Cretaceous extensional deformation with the intrusion of trachyte dykes.

D_6, D_7, D_8: End of Early Miocene – beginning of Middle Miocene stress fields with transpressional displacements due to regional rotation.

D_9: Extensional stress field with a NW–SE axis at the beginning of Late Miocene.

D_{10}: Late Miocene – Pliocene transpressional elevation in a NE–SW striking sinistral strike-slip zone with the reactivation of former structures.

The research area was divided into complex structural blocks, and a tectonic map was constructed with the larger fracture zones and the foliation strips. A structural evolution model was outlined concerning the situation of the blocks — namely, that the different foliation strips and blocks, being next to one another, can be explained by either folding or strike-slip movements, or the combination of these (Figure 14, d).

References — Irodalom

ANDERSON, E. M. 1951. *The dynamics of faulting*. – Oliver & Boyd, Edinborogh, 2nd edition, 206 p.

ANGELIER, J. 1984: Tectonic analysis of fault data sets. – *Journal of Geophysical Research* 89 (B7), pp. 5835–5848.

BALLA Z., DUDKO A., FÖLDVÁRI M., GYALOG L., HORVÁTH I., JÁMBOR Á., KIRÁLY E., KOLOSZÁR L., KOROKNAI B., MAROS GY., MARSI I., PEREGI ZS. , HARANGI SZ., LELKESNÉ FELVÁRI GY. 2003a: Kis és közepes radioaktivitású atomerőművi hulladékok végleges elhelyezése. Földtani zárójelentés (in Hungarian: Final disposal of the low- and intermediate-level waste from nuclear power plant. Conclusive geological report). – *Manuscript,* Geological Institute of Hungary, Budapest.

BALLA Z., ALBERT G., CHIKÁN G., DUDKO A., FODOR L., FORIÁN-SZABÓ M., FÖLDVÁRI M., GYALOG L., HAVAS G., HORVÁTH I., JÁMBOR Á., KAISER M., KOLOSZÁR L., KOROKNAI B., KOVÁCS-PÁLFFY P., MAROS GY., MARSI I., PALOTÁS K., PEREGI ZS., RÁLISCH L.-NÉ, ROTÁRNÉ SZALKAI Á., SZŐCS T., TÓTH GY., TURCZI G., PRÓNAY ZS., VÉRTESY L., ZILAHI-SEBESS L., GALSA A., SZONGOTH G., MEZŐ GY., MOLNÁR P., SZÉKELY F., HÁMOS G., SZŰCS I., TURGER Z., BALOGH J., JAKAB G. and SZALAI Z. 2003b: A felszíni földtani kutatás zárójelentése, Bátaapáti (Üveghuta) [in Hungarian: Final report of the ground-based geological exploration, Bátaapáti (Üveghuta)]. – *Manuscript,* Geological Institute of Hungary, Budapest.

BALLA, Z. HORVÁTH, I., TÓTH, GY., BENEDEK, K., MEZŐ, GY., MOLNÁR, P. 2004: Hydrogeological pattern of the Bátaapáti (Üveghuta) Site [A Bátaapáti (Üveghutai)-telephely vízföldtani képe]. – *Annual Report of the Hungarian Geological Institute, 2003* (this volume).

BALOGH, K., ÁRVA-SÓS, E., BUDA, GY. 1983: Chronology of grani-

toid and metamorphic rocks of Transdanubia (Hungary). – *Anuarul Institutului de Geologie şi Geofizică* 61, pp. 359–364.

Benkovics, L., Mansy, J-L., Csontos, L. and Bergerat, F. 1997: Folding in the Abaliget road cut (Mecsek Mountains). – *Acta Geologica Hungarica* 40 (4), pp. 425–440.

Bergerat, F., Csontos, L. 1988: Brittle tectonics and paleostress-fields in the Mecsek and Villány Mountains (Hungary): correlations with the opening mechanisms of the Pannonian Basin. – *Acta Geologica Hungarica* 31 (1–2), pp. 81–100.

Castro, A., Fernández, C: 1998: Granite intrusion by externally induced growth and deformation of the magma reservoir, the example of the Plasenzuela pluton, Spain. – *Journal of Structural Geology*, 20 (9/10), pp. 1219–1228.

Chikán G., Chikán G.-né, Koloszár L., Kókai A., Marsi I., Papp P., Szalai I. 1995: Terepi előkészítő munkálatok kis és közepes radioaktivitású hulladékok elhelyezésére szolgáló telephelyek kutatásához. Objektumok földtani dokumentációja (in Hungarian: Reconnaissance field works for the exploration of sites for low- and intermediate-level radioactive waste disposal). – *Manuscript,* Geological Institute of Hungary, Budapest.

Csernüsov, I. V., Volkov, V., Mohov, A., Lapina, M., Jakusev, A. Dubinyin, A., Kogan, S., Lebegyev, V., Arakeljanc, M., Nikisina, V., Satagin, K. 2002: Jelentés a Mórágyi gránit K-Ar és Rb-Sr izotópos kormeghatározásáról (in Hungarian: Chernyshev, I. V., Volkov, V., Mokhov, A., Lapina, M., Yakushev, A. Dubinin, A., Kogan, S., Lebedev, V., Arakelyants, M., Nikishina, V., Shatagin, K. 2002: Report on the results of K–Ar and Rb–Sr isotope dating of Mórágy Granitoids). – *Manuscript,* Geological Institute of Hungary, Budapest.

Csontos, L., Bergerat, F. 1993: Reevaluation of the Neogene brittle tectonics of the Mecsek–Villány area (SW Hungary). – *Annales Universitatis Scientiarum Budapestiensis Rolando Eötvös Nominatae, Sectio Geologica* 29, pp. 3–12.

Csontos, L., Benkovics, L., Bergerat, F., Mansy, J-L., Wórum, G. 2002: Tertiary deformation history from seismic section study and fault analysis in a former European Tethyan margin (the Mecsek–Villány area, SW Hungary). – *Tectonophysics* 357 (1–4), pp. 81–102.

Fodor, L., Csontos, L., Bada, G., Györfi, I., Benkovics, L. 1999: Tertiary tectonic evolution of the Pannonian basin system and neighbouring orogens: a new synthesis of paleostress data. In: Durand, B., Jolivet, L., Horváth, F., Séranne, M. (eds): The Mediterranean Basins: Tertiary extension within the Alpine Orogen. – *Geological Society, London, Special Publications* 156, pp. 295–334.

Gulácsi Z. 2003: Az Üh–25, Üh–26, Üh–27, Üh–28 és Üh–36 jelű fúrások makroszkóposan észlelhető metamorf bélyegei (in Hungarian: Macroscopic metamorphic features of Boreholes Üh–25, Üh–26, Üh–27, Üh–28, and Üh–36). – *Manuscript,* Geological Institute of Hungary, Budapest.

Gyalog L., Jámbor Á., Kókai A., Maros Gy., Peregi Zs., Konrád Gy., Máthé Z., Szebényi G. 2003: A bátaapáti A1 és A2 árok földtani leírása (in Hungarian: Geological description of Trenches A1 and A2 near Bátaapáti). – *Manuscript,* Geological Institute of Hungary, Budapest.

Hámos G. (ed.) 1999: A Bodai Aleurolit Formáció Minősítésének rövidtávú programja. Kutatási zárójelentés, 3. kötet. Földtani dokumentációs munkák a BAF megismerésére (in Hungarian: Short-term program for the qualification of the Boda Aleurolite Formation. Final Report, Volume 3, Geological documentation for the cognition of the Boda Aleurolite Formation). – *Manuscript,* Mecsekérc Környezetvédelmi Rt., Pécs.

Király, E., Koroknai, B. 2004: Magmatic and metamorphic evolution of the north-eastern Mórágy Block. (A Mórágyi-rög ÉK-i részének magmás és metamorf fejlődéstörténete). – *Annual Report of the Hungarian Geological Institute, 2003* (this volume).

Kleb, B. 1973: Geologie des Pannons im Mecsek. – *Annals of the Geological Institute of Hungary* 53 (3), pp. 743–943.

Kókai A., Sieglné Farkas Á. 2001: Töréshossz mérések a Mórágyi Komplexum feltárásaiban (in Hungarian: Fracture length measurements in outcrops of the Mórágy Complex). – *Manuscript,* Geological Institute of Hungary, Budapest.

Konrád Gy. 1998: Jelentés a Bodai Aleurolit Formáció 1995–1998. évi kutatásáról (in Hungarian: Report of the 1995–1998 research of the Boda Aleurolite Formation). – *Manuscript,* Mérce Bt., Pécs.

Koroknai B. 2003: Az irányított minták mikrotektonikai vizsgálata és összefoglaló értékelése (in Hungarian: Microtectonicstudy and summarising evaluation of the oriented samples). – *Manuscript,* Geological Institute of Hungary, Budapest.

Lelkes-Felvári, Gy., Árkai, P., Frank, W., Nagy, G. 2000: Late Variscan ultramylonite from the Mórágy Hills, SE Mecsek Mts., Hungary. – *Acta Geologica Hungarica* 43 (1), pp. 65–84.

Maros, Gy., Palotás, K. 2000a: Evaluation of planar features in Boreholes Üveghuta Üh–22 and Üh–23 with CoreDump software (Az üveghutai Üh–22 és Üh–23 fúrásban észlelt síkszerű jelenségek értékelése CoreDump szoftverrel). – *Annual Report of the Geological Institute of Hungary, 1999*, pp. 315–340.

Maros, Gy., Palotás, K. 2000b: Evaluation of the relative time series of events observed in Boreholes Üh–22 and Üh–23 near Üveghuta with CoreTime software (Az üveghutai Üh–22 és Üh–23 fúrásban észlelt események idősorrendjének értékelése CoreTime szoftverrel). – *Annual Report of the Geological Institute of Hungary, 1999*, pp. 341–352.

Maros, Gy., Pásztor, Sz. 2001: New and oriented core evaluation method: ImaGeo. – *European Geologist* 12, pp. 40–43.

Maros Gy., Balla Z., Dudko A., Fodor L., Forián-Szabó M., Koroknai B., Lantos M., Palotás K. 2003: Az atomerőművi kis és közepes aktivitású radioaktív hulladékok végleges elhelyezésére irányuló program. Felszíni földtani kutatás. Tektonikai zárójelentés (in Hungarian: Program for the final disposal of low and intermediate level radioactive waste. Ground-based exploration. Tectonic final report). – *Manuscript,* Geological Institute of Hungary, Budapest.

Maros, Gy., Palotás, K., Fodor L., Sallay E., Rálischné Felgenhauer E., Koroknai, B., Matyikó M. 2000: A Bodai Aleurolit Formációban mélyült D–5 és D–6 fúrások ImaGeo magszkennerrel történt értékelésének eredményei (in Hungarian: The results of ImaGeo core scanner analysis of Boreholes D–5 and D–6 drilled in the Boda Aleurolite Formation). – *Manuscript,* Geological Institute of Hungary, Budapest.

Márton, E., Márton, P. 1999: Tectonic aspects of a palaeomagnetic study on the Neogene of the Mecsek Mountains. – *Geophysical Transactions* 42 (3–4), pp.159–180.

Némedi Varga Z. 1983: A Mecsek hegység szerkezetalakulása az alpi hegységképződési ciklusban (in Hungarian, with English abstract: Structural history of the Mecsek Mountains in the Alpine orogenic cycle). – *Annual Report of the Geological Institute of Hungary, 1981*, pp. 467–484.

Pitcher, W. S. 1997: *The Nature and Origin of Granite.* – Chapman and Hall, London, 387 p.

Szongoth G., Zilahi-Sebess L., Galsa A., Bánné Győri E., Lendvay P., Bartha Z. 2003: Mélyfúrás-geofizikai adatok in-

tegrált értelmezése (az 1996–2003-ban végzett összes mérés alapján). Kis és közepes radioaktivitású atomerőművi hulladékok végleges elhelyezése [in Hungarian: Integrated interpretation of well-logging data (on the basis of all measurements done in 1996–2003) Final disposal of low and intermediate level radioactive waste]. – *Manuscript,* Geological Institute of Hungary, Budapest.

TARI, G. 1993: Late Neogene transpression in the Northern Imbricates Zone, Mecsek Mountains, Hungary. – *Annales Universitatis Scientiarum Budapestiensis Rolando Eötvös Nominatae, Sectio Geologica* 29, pp. 165–187.

TÜSKE T. 2001: A Mórágyi-rög metamorfitjainak szerkezeti értékelése (in Hungarian: Structural evaluation of the metamorphic rocks of the Mórágy Hills). – *Manuscript,* MSc thesis, Eötvös Loránd University, Budapest.

VÉRTESY L., CSABAFI R., FEJES I., GACSÁLYI M., GULYÁS Á., HEGEDŰS E., KISS J., KOVÁCS A. CS., KOVÁCS P., MADARASI A., PATAKY P., PRÓNAY ZS., RÁNER G., REDLERNÉ TÁTRAI M., SŐRÉS L., SZABÓ Z., TÓTH Z., TÖRÖK I., TÖRÖS E., ZILAHI-SEBESS L. 2003: A kis és közepes radioaktivitású erőművi hulladékok tervezett üveghutai tárolójával kapcsolatos, ELGI által 2003-ban végzett geofizikai munkálatok. Integrált geofizikai értelmezés 3 (in Hungarian: Geophysical work carried out by ELGI in 2003 in connection with the Üveghuta Site for low- and intermediate-level activity radioactive waste disposal. Integrated geophysical interpretation 3). – *Manuscript,* Geological Institute of Hungary, Budapest.

VÉRTESY L., GULYÁS Á., FEJES I., KOVÁCS P., KOVÁCS A. CS., PATAKY P., PRÓNAY ZS., SZABÓ Z., ZILAHI-SEBESS L. 2003b: A kis és közepes radioaktivitású erőművi hulladékok tervezett üveghutai tárolójával kapcsolatos, ELGI által 2003-ban végzett geofizikai munkálatok. Integrált geofizikai értelmezés 2 (in Hungarian: Geophysical work carried out by ELGI in 2003 in connection with the Üveghuta Site for low- and intermediate-level activity radioactive waste disposal. Integrated geophysical interpretation 2).– *Manuscript,* Geological Institute of Hungary, Budapest.

WÉBER B. 1977: Nagyszerkezeti szelvényvázlat a Ny-Mecsekből (in Hungarian, with German abstract: Grosstektonische profilskizze aus dem westlichen Mecsek-Gebirge). – *Földtani Közlöny* 107 (1), pp. 27–37.

WEIN GY. 1965: Az Északi Pikkely a Mecsek hegységben (in Hungarian: Northern Imbricate in the Mecsek Mountains). – *Bányászati Lapok* 98 (6), pp. 402–411.